Annu. Rev. Fluid Mech. 1994. 26 : 65–102

DYNAMICS OF DROP DEFORMATION AND BREAKUP IN VISCOUS FLUIDS

Howard A. Stone

Division of Applied Sciences, Harvard University, Cambridge, Massachusetts 02138

KEY WORDS: capillary instability, satellite drops, chaotic flows, surfactants, tip streaming

1. INTRODUCTION

This article describes the dynamics of drop deformation and breakup in viscous flows at low Reynolds numbers. An attempt has been made to bring together a wide range of studies in the drop deformation literature, as well as to provide a large number of references to potential applications. In particular, a summary is provided of experimental, numerical, and theoretical investigations that examine drop breakup in externally-imposed flows, e.g. uniaxial extensional fluid motion or more complicated time-periodic flows. For well-characterized flow conditions that lead to breakup, the effects of flow and material parameters on the drop size distribution are summarized. Also, a short discussion is given of the stability of the shapes of translating drops.

The subject of deformation of neutrally buoyant drops in viscous shear flows at low particle Reynolds numbers was summarized by Acrivos (1983) and was reviewed in this series by Rallison (1984). The Acrivos and Rallison papers present (*a*) theoretical descriptions of steady, nearly spherical shapes and steady, long slender shapes, (*b*) a description of efficient boundary integral numerical methods, and (*c*) a summary of the experimental work performed prior to 1984. As documented in these review articles, many of the important ideas necessary for understanding drop

0066–4189/94/0115–0065$05.00

deformation can be traced to three articles by G. I. Taylor (1932, 1934, 1964).

During the past ten years there have been several notable advances in the understanding of drop dynamics in well-characterized flow fields. Not only have several gaps in the literature been filled, while the limits of existing theoretical predictions based upon small (nearly spherical) and large (slender body) deformation analyses have been clarified, but the recent investigations have focused upon several new problems (e.g. breakup) and physical influences (e.g. surfactants and complex flows). Our goal here is to provide the reader with an understanding of these recent studies that focus upon drop breakup.

We will first outline the problem area (Section 2) and describe experimental studies that contribute to an improved understanding of drop deformation in shear flows (Section 3). Inevitably there is overlap with the Acrivos and Rallison review articles, which is necessary for this review to be self-contained. Section 4 provides a discussion of different aspects of the drop breakup problem, including an overview of effects introduced by flows more complicated than steady shear flow. Section 5 describes a number of studies examining the influences of surfactants on the degree of drop deformation and breakup and implications for tip streaming.

Section 6 gives a discussion of the low Reynolds number buoyancy-driven translation of nonspherical drops. As is well known (Batchelor 1967), an initially spherical drop is a steady solution to the Stokes equations, independent of the magnitude of the interfacial tension. However, only recently has the *stability* of this solution been investigated. Indeed, translating drops may assume highly distorted shapes with long tails or large cavities. All research, however, has focused on either of the driving forces of buoyancy or imposed shear acting alone, and a quantitative study of the dynamics when the buoyancy and shearing motions are comparable has not been reported.

There are a number of topics with connection to drop deformation in viscous flows that cannot be discussed because of lack of space. For example, drop breakup in electric and magnetic fields, the effect of multiple particles or nearby boundaries, non-Newtonian effects, and high Reynolds number motions are all outside the scope of this review.

In all the results presented in this paper, the degree of drop deformation and the character of the breakup are largely determined by the magnitude of interfacial tension stresses relative to the magnitude of the flow-generated viscous stresses. Some frequently mentioned applications which motivate, or serve as extensions of, many of the studies of drop deformation and breakup are summarized in Table 1. The typical problems span a wide variety of length scales, from the submicron scale to hundreds

Table 1 Typical applications for which a drop deformed or fragmented in an extensional flow is a useful prototype

Application	Reference
Dispersion of color concentrates	Grace (1971)
Processing of microscale dispersions such as margarine and ice cream	de Bruijn (1989)
Mixing in multiphase viscous systems	Ottino (1990), Meijer & Janssen (1993)
Blending of molten polymers	Elemans (1989)
Emulsion formation and rheology	Han (1981)
Ink-jet printers	Döring (1982)
Viscous sintering (cohesion) of adjacent fluid regions	Kruiken (1990)
Deformation of biological cells	Greenspan (1978), Zinemanas & Nir (1988)
Deformation of liquids encapsulated inside elastic membranes	Li et al (1988), Skalak et al (1989)
Manufacture of two-phase glass	Seward (1974)
Drawing of glass sheets	Wilmott (1989a)
Measurement of interfacial tension from time-dependent shape changes	Elemans et al (1990), Carriere et al (1989), Tjahjadi et al (1993)
Stretching of viscous inclusions in geophysical studies of mantle dynamics	Spence et al (1988)

of kilometers, hence provide a common theme for discussion among fluid dynamicists interested in a variety of applications.

2. PROBLEM DESCRIPTION AND GOVERNING EQUATIONS

The prototypical two-phase flow problem we wish to consider consists of a drop of Newtonian fluid of density $\rho-\Delta\rho$ and viscosity $\lambda\mu$ suspended in an unbounded Newtonian fluid, density ρ and viscosity μ (Figure 1). The undeformed radius of the drop is denoted by a. The interfacial tension acting between the two fluid phases is denoted by γ and may vary along the interface S owing to a nonuniform temperature or the presence of a nonuniform distribution of surfactants with surface concentration Γ. In the presence of surfactant (or temperature) gradients, an equation of state $\gamma(\Gamma)$ must also be introduced, though other possible rheological influences of surfactant are neglected (e.g. surface elasticity; see Edwards et al 1991).

At low Reynolds numbers, fluid motion is governed by the Stokes and continuity equations, which have the dimensionless form ($\hat{}$ denotes drop fluid variables)

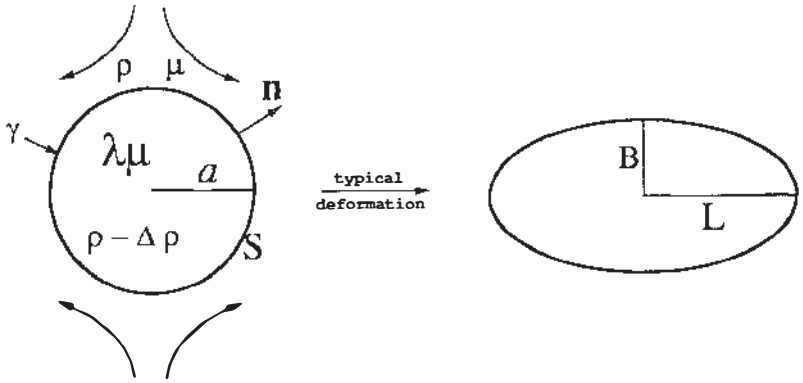

Figure 1 Schematic of drop deformation in a straining flow.

$$\nabla^2\mathbf{u} = \nabla p, \quad \nabla^2\hat{\mathbf{u}} = \nabla\hat{p},$$
$$\nabla\cdot\mathbf{u} = 0, \quad \nabla\cdot\hat{\mathbf{u}} = 0, \tag{1}$$

where the pressure p is the dynamic pressure (i.e. the actual fluid pressure minus the background hydrostatic pressure). All distances are scaled by a, velocities are scaled by u_c, which depends on the nature of the forcing present in the problem, and pressures are scaled by $\mu u_c/a$ and $\lambda\mu u_c/a$, respectively, outside and inside the drop.

Continuity of velocity requires $\mathbf{u} = \hat{\mathbf{u}}$ along the fluid-fluid interface S. Viscous and pressure stresses generated by the fluid motion tend to deform the drop while interfacial tension stresses tend to resist deformation. The dimensionless form of the stress boundary condition depends on the specific problem of interest and the choice of the characteristic velocity scale. In addition to the viscosity ratio λ, two dimensionless parameters typically appear in the stress boundary conditions:

$$\mathsf{C} = \frac{\mu u_c}{\gamma} \quad \text{and} \quad \mathsf{B} = \frac{\Delta\rho g a^2}{\gamma}, \tag{2}$$

where g is the gravitational acceleration. The capillary number C represents a measure of viscous stresses relative to interfacial tension stresses and the Bond number B represents typical hydrostatic pressure variations relative to interfacial tension stresses.

Fluid motions internal and external to the drop arise from one of four sources:

1. An externally-imposed velocity field $\mathbf{u}^\infty(\mathbf{x})$ at large distances from the drop, with typical shear rate G in the neighborhood of the drop. With

$u_c = Ga$, the stress boundary condition, for constant γ is

$$\mathbf{n}\cdot\mathbf{T} - \lambda\mathbf{n}\cdot\mathbf{T} = \frac{1}{\mathrm{C}}(\nabla_s\cdot\mathbf{n})\mathbf{n} - \frac{\mathrm{B}}{\mathrm{C}}\hat{\mathbf{g}}\cdot\mathbf{x}\mathbf{n} \quad \text{on } S, \tag{3}$$

where $\mathbf{T}$ is the stress tensor defined in terms of the dynamic pressure, $\mathbf{n}$ is the unit normal directed outward from the drop, $\nabla_s\cdot\mathbf{n}$ is the local interface curvature, $\hat{\mathbf{g}}$ denotes a unit vector in the direction of gravity and $\mathbf{x}$ denotes the position vector measured relative to the drop center. Theoretical and numerical studies in this limit have been restricted to neutrally buoyant drops ($\mathrm{B} = 0$).

2. A deformed drop for which the finite interfacial tension generates a flow. Here the fluid is assumed quiescent at large distances, so that with $u_c = \gamma/\mu(1+\lambda)$ the normal stress balance takes the form

$$\mathbf{n}\cdot\mathbf{T} - \lambda\mathbf{n}\cdot\hat{\mathbf{T}} = (1+\lambda)(\nabla_s\cdot\mathbf{n})\mathbf{n} - (1+\lambda)\mathrm{B}\hat{\mathbf{g}}\cdot\mathbf{x}\mathbf{n} \quad \text{on } S. \tag{4}$$

If we introduce the viscosity ratio into the definition of the characteristic velocity, the larger fluid viscosity controls the typical drop deformation rate (Rallison 1984). The classical capillary breakup of an infinite fluid thread provides a common example where interfacial tension is the driving force for motion and causes amplification of disturbances with wavelength greater than the thread circumference, eventually leading to fragmentation of the thread into a series of drops. Hence, comparing cases (1) and (2), it is apparent that interfacial tension has different dynamical influences at different stages of the drop breakup process.

3. Buoyancy-driven motions in an otherwise quiescent fluid. Here the fluid is assumed quiescent at large distances and with $u_c = \Delta\rho g a^2/\mu(1+\lambda)$ (alternatively one can use the Hadamard-Rybcyński rise speed of a drop in an infinite fluid which simply changes u_c by a constant), the normal stress balance is

$$\mathbf{n}\cdot\mathbf{T} - \lambda\mathbf{n}\cdot\hat{\mathbf{T}} = \frac{1+\lambda}{\mathrm{B}}(\nabla_s \tag{5}$$

4. Flows either produced or affected by interfacial tension variations (Marangoni motions) caused by temperature variations and/or the presence of surfactants (e.g. see Levich & Ḳrylov 1969). A typical velocity induced by variations in interfacial tension has magnitude $u_c = \Delta\gamma/\mu(1+\lambda)$, where $\Delta\gamma$ characterizes the initial variation in interfacial tension. A tangential stress imbalance occurs along the surface and, appropriately nondimensionalized, $-\nabla_s\gamma$ must be added to the right-hand side of Equations (3–5). The effects of surfactants on deformation and breakup in extensional flows are summarized in Section 5.

The problem statement is completed by the kinematic condition, which we may write as $dS/dt = \mathbf{u} \cdot \mathbf{n}$ for points on the interface.

In case (1) most research has focused on neutrally buoyant drops immersed in locally linear flows $\mathbf{u}^{\infty}(\mathbf{x}) = \boldsymbol{\Gamma} \cdot \mathbf{x}$, where $\boldsymbol{\Gamma}$ is a second order tensor characterizing the local velocity gradient. This flow approximation is expected to be representative of many applications so long as the largest dimension of the drop is smaller than the typical scale over which variations of the velocity gradient occur. The components of $\boldsymbol{\Gamma}$ in the neighborhood of the drop must be specified, which requires specifying the ratio of the local rate-of-strain to the local vorticity of the applied fluid motion. Any time-dependence of the external flow must also be specified. This *flow-type* classification is important for characterizing the degree of drop deformation (Section 3).

Recent studies have considered the case of time-periodic flow fields, defined over dimensions much larger than a typical drop size (see Section 4). Such a flow is globally more complicated than a linear flow, but even in such circumstances the local flow field in the neighborhood of the drop is often well-approximated by a linear flow with a time-dependent velocity gradient tensor $\boldsymbol{\Gamma}(t)$.

The *initial drop shape* is important for completely characterizing drop dynamics in either shear flows or buoyancy-driven motions and, in particular, plays an important role for determining whether or not transient effects eventually lead to breakup. From the standpoint of applications this is not as restrictive as it may first appear since the details of the shape are typically not important, but rather it is the initial degree of deformation (whether the drop begins nearly spherical or as a highly extended thread)—information which is expected to be available—that is relevant.

In order to characterize the degree of drop distortion it is convenient for modest shape changes to use the deformation parameter $D = (L-B)/(L+B)$, where $2L$ and $2B$ are the drop length and breadth, respectively ($0 \leq D < 1$). For more highly extended drop shapes, a dimensionless length L/a is an appropriate measure of deformation (Figure 1). A complete description of configurations in shear flows also necessitates knowledge of the drop's orientation relative to say the principal axes of strain of the imposed flow (for example, see Rallison 1984).

The Reynolds numbers for the fluid motions considered here are assumed small so that we require $\rho a u/\mu \ll 1$ in both fluid phases, where u is chosen as the largest velocity characteristic of the fluid motion. For the majority of our discussion, drops are to be considered neutrally buoyant, $\Delta\rho = 0$, though in Section 6, drop deformation is a consequence of fluid motion associated with buoyancy. We will summarize those aspects of the

flow problems (1)–(4) concerned with steady isolated drop shapes, transient deformation, breakup in simple and complex flows, and surfactant effects.

3. STEADY DROP DEFORMATION IN LINEAR FLOWS

An excellent discussion of drop deformation, including experimental observations and theoretical predictions of steady drop shapes and orientations, is provided by Rallison (1984) and is not reviewed here. In this section we describe qualitatively the dependence of the degree of drop deformation on the viscosity ratio. We also summarize recent experimental observations spanning a wide range of flow conditions, which add substantially to the understanding of the steady state deformation problem and the prediction of the critical capillary number for breakup as a function of the viscosity ratio and flow type. Effects of surfactants are discussed in Section 5.

Qualitative Features of Deformation

When a neutrally buoyant drop is placed in a shear flow it will deform. For all viscosity ratios, the drop shape will be nearly spherical provided the capillary number is sufficiently small. In this limit a small deformation analysis is valid and predicts the drop shape $D(\mathsf{C})$ and orientation in the flow (e.g. see Figures 2 and 3).

When $\mathsf{C} \ll 1$, the deformation D is linear in C, as first demonstrated by Taylor (1932). In particular, $D = (19\lambda+16)\mathsf{C}/(16\lambda+16)$ for an axisymmetric extensional flow, which shows that the effect of the viscosity ratio λ is small. Even if $\mathsf{C} > O(1)$, a drop will maintain a nearly spherical shape provided $\lambda \gg 1$ *and* the imposed flow has sufficient vorticity so that the drop fluid spins almost as a rigid body. On the other hand, for low viscosity ratios, $\lambda \ll 1$, the application of a sufficiently large shear rate ($\mathsf{C} \gg 1$) forms steady, highly elongated slender drop shapes with nearly pointed ends.

As the capillary number is increased the drop becomes increasingly elongated. The critical capillary number for breakup, C_c, corresponds to the smallest steady shear rate G_c for which the drop, beginning with a nearly spherical shape, is unable to maintain a steady shape and consequently undergoes a transient, continuous stretching. The drop attains a thread-like shape and eventually breaks into smaller drops. The rate of transient stretching is controlled by the larger of the two fluid viscosities. The actual fragmentation of the thread into small drops is described in Section 4.

Prior to the transient stretching and breakup, drops are characterized by their maximum deformation for capillary numbers slightly below C_c. For $\lambda > 0.1$, the maximum steady ellipsoidal deformation is rather modest

and for viscosity ratios greater than about 5 the final steady shapes prior to breakup are not very different from a sphere. Proceeding beyond the linear small deformation analysis in order to describe these more distorted shapes is straightforward in principle, but, in practice, is rather difficult algebraically. The higher order analysis for nearly spherical distortions is developed by Barthès-Biesel & Acrivos (1973) and summarized by Rallison (1980). Comparisons of the predictions of small deformation theory with experiments and numerical simulations, including the variation of C_c with viscosity ratio and flow-type Γ, are typically quite good for $\lambda > 0.1$. On the other hand, for $\lambda < 0.01$, slender body theory (Hinch & Acrivos 1979) predicts the drop shapes and critical capillary number with typical errors less than 20% (Bentley & Leal 1986b).

The effect of vorticity of the external flow plays a critical role in determining whether or not drop breakup is possible in a shear-type flow. This fact was recognized by Taylor (1934), who showed that if $\lambda > 4$, and the drop begins with a nearly spherical shape, drop breakup is not possible in a simple shear flow, independent of the magnitude of the shear rate. In this case, it is not possible to deform a drop beyond a modest distortion, so that upon application of higher shear rates the deformation remains unchanged and the drop fluid simply circulates faster. Breakup, however, is always possible in a planar extensional flow for any viscosity ratio λ. A pure extensional flow is, of course, one with zero vorticity, while a simple shear flow is special in that it has equal parts vorticity and strain rate.

This *flow-type* effect provides a dramatic example of the role of vorticity for inhibiting drop breakup. For a simple shear flow, drops become more susceptible to breakup for $\lambda < 4$ due to a coupling of deformation and orientation in the flow: At lower viscosity ratios (but comparable capillary numbers) drops remain oriented closer to the extensional axis of the shear flow (Rumscheidt & Mason 1961, Bentley & Leal 1986b) and, hence, experience a stronger flow; as the shear rate increases, increased deformation thus occurs to a larger degree for small viscosity ratios eventually leading to breakup.

Because of experimental difficulties, experimental investigations of flows intermediate to simple shear and two-dimensional extensional flow—flows that have variable ratios of vorticity to strain rate—were investigated only recently and are now summarized.

Deformation and Critical Capillary Number in Linear Flows With Vorticity

Bentley & Leal (1986a,b) used a computer-controlled four-roll mill to study drop deformation experimentally in the undisturbed two-

dimensional linear flow

$$\mathbf{u}^{\infty}(\mathbf{x}) = \boldsymbol{\Gamma}\cdot\mathbf{x} \quad \text{where} \quad \boldsymbol{\Gamma} = \frac{G}{2}\begin{pmatrix} 1+\alpha & 1-\alpha & 0 \\ -1+\alpha & -1-\alpha & 0 \\ 0 & 0 & 0 \end{pmatrix}. \tag{6}$$

The velocity gradient tensor $\boldsymbol{\Gamma}$ is known by specifying the shear rate G and a flow-type parameter α. The ratio of vorticity to strain rate in these flows is given by $(1-\alpha)/(1+\alpha)$ and is controlled independent of G. Simple shear flow corresponds to the limit $\alpha = 0$, while a two-dimensional irrotational flow has $\alpha = 1$. The four-roll mill was first used by Taylor (1934) for drop deformation studies, and was also utilized in a large number of studies by Mason and coworkers (e.g. Rumscheidt & Mason 1961). The particular flow described by Equation (6) has been studied in detail by Giesekus (1962). With the exception of an experimental study by Hakimi & Schowalter (1980) that was confined to vorticity dominated flows, and hence limited to the study of small drop deformations only, all experimental studies prior to 1986 were concerned with either simple shear or two-dimensional extensional flows.

Owing to the implementation of a computer-control strategy, hence a degree of patience not possible in earlier experiments, Bentley & Leal's study provides a wealth of experimental data. Improved data were obtained for extensional flows, especially for viscous drops which require considerable times to deform. It should be noted that previous extensional flow experiments, and all published plots summarizing the dependence of the critical shear rate on viscosity ratio (e.g. Grace 1971) report that the critical capillary number for breakup C_c increases for larger viscosity ratios, $\lambda > O(1)$. However, the Bentley & Leal study clarified that, in fact, C_c remains nearly constant for $\lambda > 5$ (see Figure 4). It appears that earlier studies probably did not wait long enough to establish a steady state, as such waiting times can be $O(\mu a/\gamma)$ which is quite long for high viscosity ratio drops.

Specifically, Bentley & Leal's (1986b) investigation includes:

1. Comparison of small deformation and slender body theories with steady state experiments covering a wide-range of viscosity ratios and flow-types, $10^{-3} < \lambda < 10^{2}$ and $0.2 \leq \alpha \leq 1$.
2. Measurements of the critical capillary number and critical degree of drop deformation for breakup as a function of λ and α, i.e. $\mathsf{C}_c(\lambda,\alpha)$ and $D_c(\lambda,\alpha)$.

We now briefly examine typical results for low and high viscosity ratio drops.

LOW VISCOSITY RATIOS For small viscosity ratios, $\lambda \ll 1$, the largest steady drop shapes are long and slender, provided that the applied shear rate is sufficiently large. In this limit some simple scaling arguments are possible (Acrivos 1983). In particular, if the slender drop has volume V, steady length $2L$, and a narrow breadth εL ($\varepsilon \ll 1$), then conservation of mass requires $2\pi\varepsilon^2 L^3 = O(V = 4\pi a^3/3)$. An applied shear rate G exerts a viscous stress μG along the interface, whose normal component must be balanced by the interfacial stress $\gamma/(\varepsilon L)$. Combining these two arguments yields an estimate for the slenderness $\varepsilon = \mathsf{C}^{-3}$ and a steady dimensionless half-length $L/a = O(\mathsf{C}^2)$, where we continue to use the definition $\mathsf{C} = \mu G a/\gamma$. Hence, slender shapes ($\varepsilon \ll 1$) require large capillary numbers, $\mathsf{C} \gg 1$. These arguments suggest that for an air or vapor bubble ($\lambda = 0$) of uniform internal pressure, a stable steady shape is always possible and indeed detailed analysis and experiments show this to be true.

However, for a steady shape of a low viscosity ratio drop ($\lambda \ll 1$) exposed to a high shear rate G, an internal pressure gradient $\Delta p/L \approx \lambda\mu(GL)/(\varepsilon L)^2$ is required to push the fluid from the end of the drop back towards the center with typical speed GL. As the magnitude of the pressure gradient is $\gamma/(\varepsilon L)$, we see that $\lambda = O(\varepsilon^2)$ for the slenderness approximation to hold, i.e. $\lambda^{1/2} \ll 1$. Also, it follows that $\mathsf{C}\lambda^{1/6} = O(1)$, which with a more detailed analysis may be shown to be the form of a criterion for the critical capillary number necessary for breakup as a function of viscosity ratio.

In Figure 2, drop deformation as a function of capillary number is shown for $\lambda = 10^{-3}$ and two-dimensional flows corresponding to $\alpha = 0.6$ and 0.8. This figure is typical of results from the very low viscosity ratio experiments. In Figure 2*a* theoretical predictions for the drop shape are shown below the corresponding experimental photographs, while Figure 2*b* displays the deformation parameters D and L/a as functions of capillary number. For small distortions from a spherical shape, the shapes predicted by a small deformation analysis are calculated, while larger drop distortions are compared with shapes calculated using slender body analysis (Acrivos & Lo 1978).

The small deformation analysis is in reasonable agreement with the overall shape for $\mathsf{C} < 0.25$, though clearly it has a limited range of utility as it predicts unrealistic lobes (Figure 2*a*). The drop shapes become increasingly elongated as the capillary number increases, but the effect of flow type in the low viscosity ratio limit is rather small. Since the elongated drop is oriented by the flow along a direction where the effective strain rate is $G\alpha^{1/2}$, the slender body theory estimate (Hinch & Acrivos 1979) of the critical capillary number is modified to read $\mathsf{C}_c\lambda^{1/6} = 0.145/\alpha^{1/2}$, which is in good agreement with the data. Overall, slender body theory generally lies within 20% of the experiment results for the most highly deformed drops.

The most distorted drop shapes provide a vivid example of nearly pointed ends which may arise even in systems with finite interfacial tension. Two-dimensional free-surface experiments and theory illustrate that cusp-like shapes are indeed possible even if $\mathsf{C} = O(1)$; the reader is referred to Jeong & Moffatt (1992) and Joseph et al (1991). The analysis has not been extended to three dimensions but it appears that for a low viscosity ratio drop the end is not a cusp, and appears on the macroscale to be sharp (i.e. there is a finite but very large curvature; see also Buckmaster 1972 and Sherwood 1981).

For the large distortions typical of low viscosity ratio drops it is reasonable to question the validity of the linear flow approximation. Sherwood (1984), motivated by Taylor's (1934) experimental observation of tip streaming of small droplets from the end of stretched drops, has addressed the effect of higher order terms in the undisturbed flow field within the context of a slender body analysis. Cubic terms in the external flow, if sufficiently strong, give rise to rapid growth at the end of the drop. Though this result may have some bearing on breakup when velocity gradients occur on the same scale as the highly distorted drop shape, there is now strong evidence that tip streaming is a consequence of surfactant gradients (Section 5; de Bruijn 1989).

HIGH VISCOSITY RATIOS In Figure 3, drop deformation is examined as a function of flow type for $\lambda = 57$. It is observed experimentally, in agreement with a prediction using the $O(\mathsf{C}^2)$ theory of Barthès-Biesel & Acrivos (1973), that for both the $\alpha = 0.2$ and $\alpha = 0.4$ flows, it is impossible to fragment the drop when beginning with a spherical shape and thus a limiting steady deformation is reached. The effect of vorticity is clearly to inhibit breakup for $\alpha \leq 0.4$. Overall, there is excellent agreement between theory and experiment, including prediction of the drop shape and the critical capillary number for onset of transient stretching, which is a precursor to eventual fragmentation.

Figure 3 is typical of the high viscosity ratio data. For drops with lower viscosity ratios, $\lambda = O(1)$, the deformation is similar to Figure 3, except that no limiting deformation is obtained when the vorticity of the undisturbed flow is increased ($0 < \alpha \leq 1$).

CRITICAL CAPILLARY NUMBER VS VISCOSITY RATIO AND FLOW TYPE Figure 4 shows the critical capillary number for breakup (i.e. the onset of continuous deformation) as a function of viscosity ratio. All data for two-dimensional flows spanning simple shear to planar extensional flow are presented. The solid and dashed curves indicate theoretical predictions based upon small deformation theory and slender body analysis, respectively. A similar plot illustrating the maximum stable deformation as a

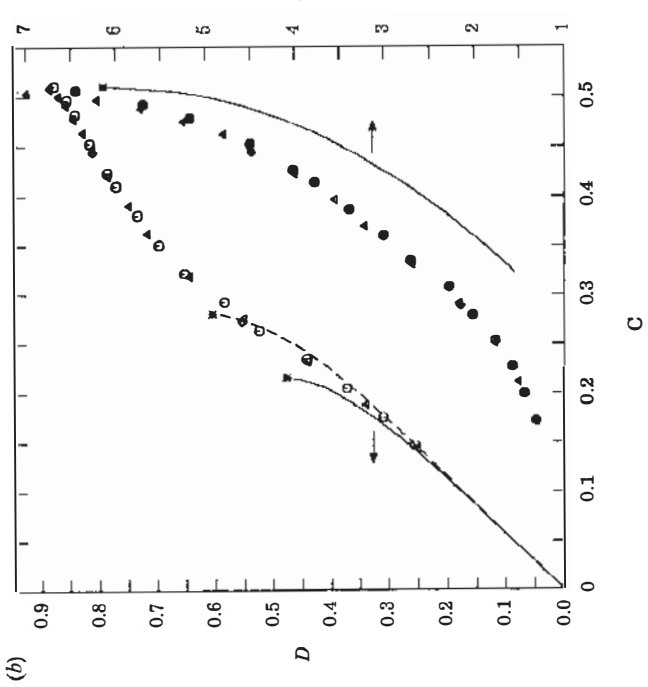

Figure 2 Drop deformation as a function of capillary number for a low viscosity ratio, $\lambda = 10^{-3}$. (*a*) $\alpha = 0.8$; theoretical predictions for the drop shape are given below the corresponding experimental photographs. Small deformation theory is used for $C < 0.27$ and slender body theory is used for $C > 0.32$. The orientation angle relative to the extensional axis is denoted by θ. (*b*) $\alpha = 0.6$; open symbols correspond to the deformation parameter D and are compared with the $O(C)$ (*solid curve*) and $O(C^2)$ (*dashed curve*) predictions of small deformation theory. The filled-in symbols correspond to the deformation parameter L/a and are compared with the predictions of slender body theory (*solid curve*). An asterisk terminating a theoretical line indicates a prediction of breakup, i.e. unsteady stretching (Bentley & Leal 1986b).

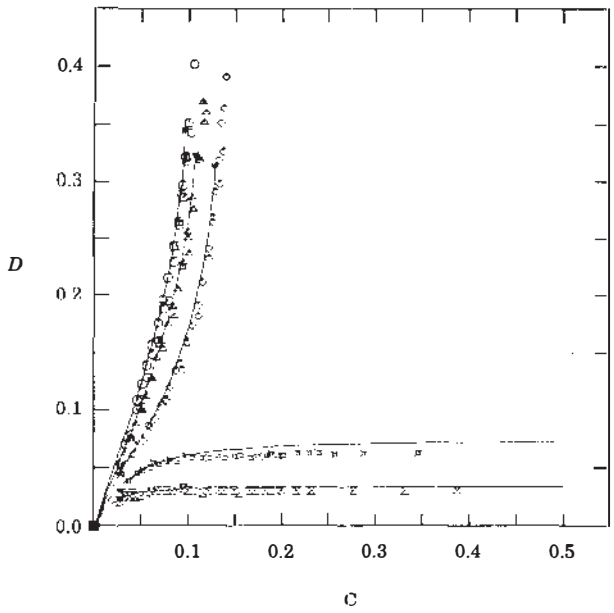

Figure 3 Drop deformation as a function of capillary number for $\lambda = 57$ and flow-types $\alpha = 1.0$ (○), 0.8 (△), 0.6 (◇), 0.4 (⊠), 0.2 (⧖). An asterisk terminating a theoretical curve indicates a prediction of breakup, i.e. unsteady stretching (Bentley & Leal 1986b).

function of viscosity ratio is given by Bentley & Leal (1986b). Overall, the very high capillary numbers necessary to produce large deformation of low viscosity ratio drops indicate that such surfactant-free drops will be difficult to fragment in a flow.

4. DROP BREAKUP

The focus of most drop dynamics research has been the prediction of the critical conditions beyond which no steady drop shape exists. A practical question from the standpoint of applications is to ask about the final state of a multiphase system, in particular what the final drop size distribution might be. Clearly, this is a formidable task. In order to develop an improved understanding, it is necessary to determine which variables control the time-dependent dynamics of drop breakup, how changes in the flow affect the drop behavior, etc. Several investigations have combined experimental and numerical studies in an attempt to answer some of these questions, though the current state of knowledge is still largely qualitative.

In this section we provide a summary of the basic modes of breakup of

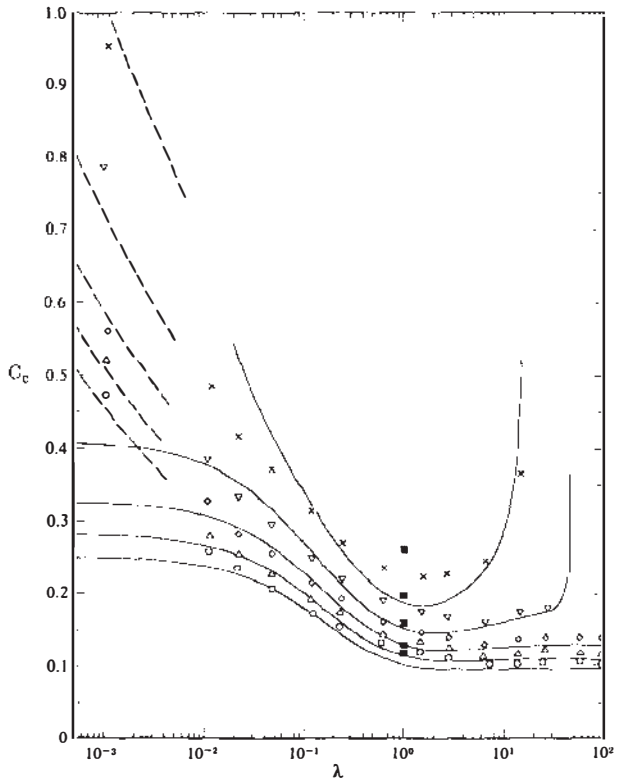

Figure 4 Effects of flow-type on the critical capillary number for drop breakup. Experimental results are presented for flow types $\alpha = 1.0$ (○), 0.8 (△), 0.6 ◇), 0.4 (▽), 0.2 (×). The solid curves are the prediction of the $O(\mathbf{C}^2)$ small deformation theory and the dashed curves are the prediction of slender body theory (Bentley & Leal 1986b). The ■ symbols are the boundary integral numerical results of Rallison (1981).

isolated drops, the effect on drop breakup of simple time-dependent flows as well as more complex (in this case chaotic) flows, the role of capillary waves during breakup, and the formation of satellite drops. A description is also given of the dynamics associated with the response of a stretchable (dumbbell-like) microstructure in time-periodic flows. Finally, time-dependent drop stretching is discussed for the case of vanishing interfacial tension, which is a limit with geophysical and material science applications.

As described in Section 3, if an initially spherical drop is placed in a weak *steady* flow, the drop deforms eventually reaching a state where the viscous and pressure forces exerted by the flow on the drop are balanced by the resistance due to interfacial tension forces. When the critical capillary

number is exceeded, the drop begins a transient elongation. The term "drop breakup" often refers to this condition, even though actual fragmentation of the droplet is rarely discussed. The drop subsequently stretches and thins, eventually reaching a thread-like shape where it stretches passively, identical to a fluid element of the undisturbed flow. There are cases in which, if the drop radius becomes small enough, capillary waves can cause the thread to fragment during flow (Mikami et al 1975, Tjahjadi & Ottino 1991), though this response requires very large elongations, typically greater than 20 times the initial drop radius. Also the drop may fragment near the middle of the thread, forming a number of smaller droplets; the details of this mode of breakup depend on the nature (and time dependence) of the externally applied flow.

The most comprehensive experimental work focusing upon drop dynamics is the study by Grace (1971), which describes model transient experiments including the use of a programmed gradual reduction of shear rate to produce drop fragmentation without significant stretching and a systematic study of the drop size distributions measured following breakup at supercritical values of the capillary number. Grace's work suggested several fundamental problems involving time-dependent effects which could provide insight into details of the breakup process. We begin our discussion of breakup with the response of a modestly deformed drop to some simple flow changes.

Time-Dependent Effects: Step Changes in Flow Conditions

Stone et al (1986) and Stone & Leal (1989a,b) present an experimental and numerical investigation of the effect of simple time-dependent flows on drops that have been stretched initially in flows at slightly supercritical values of the capillary number C_c. A computer-controlled four-roll (Bentley & Leal 1986a,b) is used to perform the experiments, which allows control over a wide range of parameters. Only step changes in the flow to subcritical conditions are examined. For flows with constant flow type (α), the experiments correspond to step reductions in shear rate, or $C(\alpha) < C_c(\alpha)$, where the notation indicates that the final value of the capillary number is less than the critical value at the specified flow type. In another series of experiments, abrupt changes of the flow type are studied, as are flows where the flow type and shear rate are changed simultaneously so long as the final state corresponds to subcritical flow conditions. Such simple flow modifications are expected to be representative of situations where rather abrupt flow changes occur (Grace 1971); for example, abrupt flow changes occur wherever the apparatus geometry changes substantially such as at entrances and exits, baffles, etc, and at the entrance to the repetitive mixing sections of a static mixer.

Breakup and the details of the drop size distribution depend on the time history of the applied flow. For example, consider the effect of an abrupt halt of the flow for a drop deformed beyond its maximum steady shape D_c with a flow at the critical capillary number. Provided the drop has been stretched sufficiently beyond D_c, then after flow stoppage, the drop first relaxes back towards a spherical shape, but subsequently fragments, forming a number of smaller droplets. Capillary wave instabilities play only a minor role for such modest extensions. This relaxation and breakup process following cessation of the flow is documented for several different viscosity ratios in Figures 5 and 6, illustrating the results of typical experiments and boundary integral calculations, respectively. The results demonstrate that (*a*) the ends of the drop become rounded and eventually pinch off from the central filament if the initial deformation is large enough, (*b*) capillary waves do not play a significant role in the dynamics for these modest extensions, and (*c*) high viscosity ratios clearly tend to inhibit the breakup process.

The breakup mechanism illustrated in Figures 5 and 6 is termed "end-pinching" and was observed previously in the experiments of Taylor (1934) and Grace (1971). Grace mentioned capillary wave instabilities as an explanation for this mode of fragmentation, though it is proper to describe the breakup of modestly deformed drops in terms of a deterministic interfacial-tension-driven flow dominated by end effects, as discussed below.

There are a number of different situations where, following an abrupt change in flow conditions, drop relaxation perhaps leading to this "end-pinching" mode of breakup is relevant. For example, the retraction of extended drops occurs following the rapid ejection of drops from a nozzle during ink-jet printing (Döring 1982); similar relaxation of finitely extended fluid drops is observed during processing of polymer composites (Carriere et al 1989).

End-pinching is a consequence of an interfacial-tension-driven flow associated with curvature variations along the surface of the finite drop. The drop attempts to return to a spherical shape, though fluid motions produced by internal pressure gradients lead to breakup. Because higher drop viscosities damp internal flows, while lower external viscosities increase the speed with which the ends of the drop retract through the surrounding fluid, it follows that higher-λ drops are able to sustain much higher initial elongations prior to breakup during the relaxation process. This behavior is clearly illustrated in Figures 5 and 6. The available experiments suggest that the maximum length needed to ensure breakup for $\lambda > 1$ increases roughly linearly with λ as the qualitative arguments above would suggest (see Stone & Leal 1989a, Figure 10).

In all the experiments reported by Stone & Leal it is possible to explain

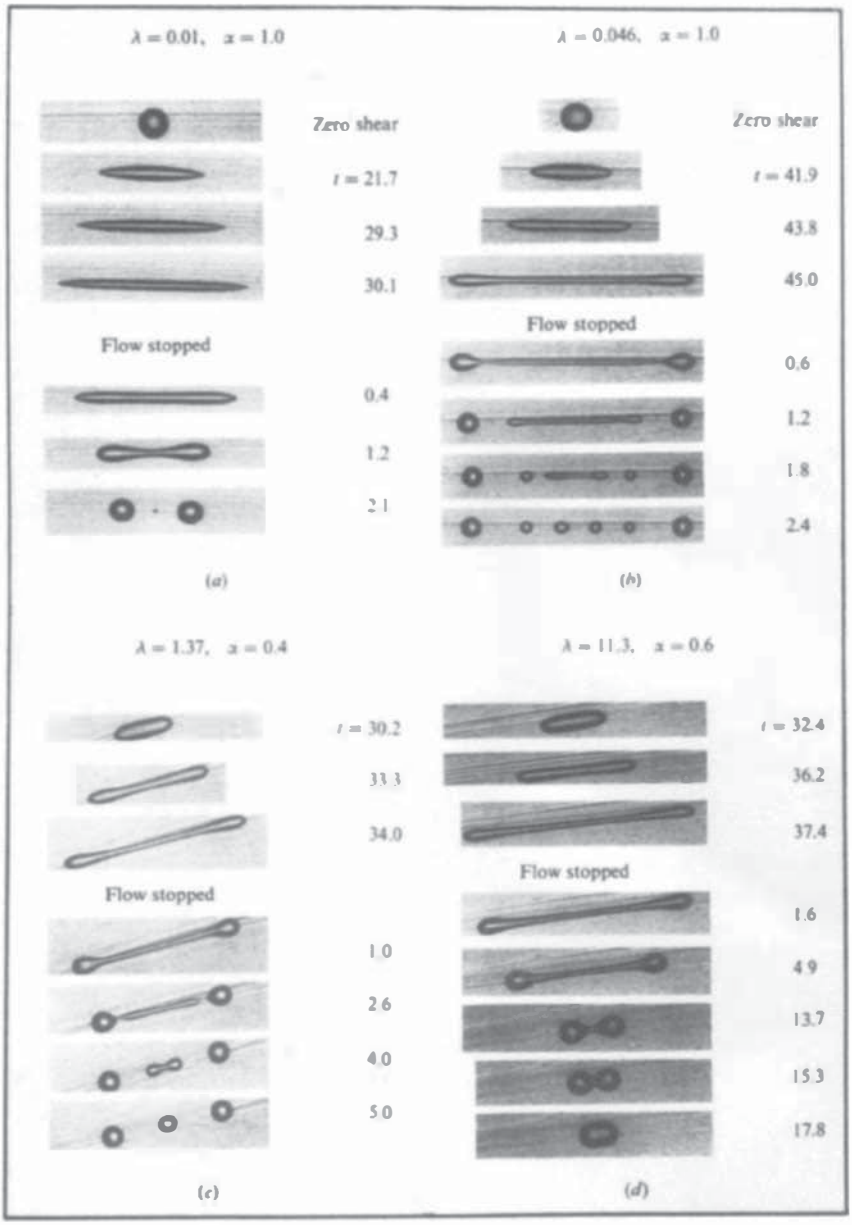

Figure 5 Experiments illustrating the effect of viscosity ratio on the relaxation and fragmentation of initially stretched drops after the flow has been stopped (Stone et al 1986).

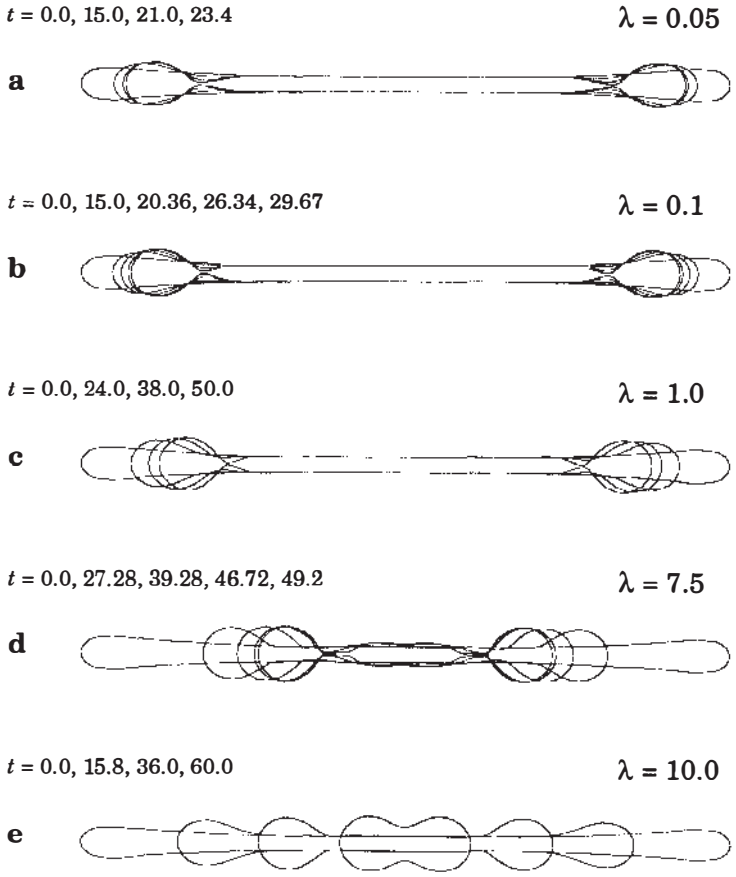

Figure 6 Numerical simulations illustrating the effect of viscosity ratio on the relaxation of initially extended drops in an otherwise quiescent fluid. The same initial shape is used in each simulation. The initial drop shape is taken from an experiment for $\lambda = 11.3$ and is similar to all experimental results for $\lambda > 0.05$ (Stone & Leal 1989a).

the qualitative and quantitative dynamics assuming the interfacial tension is constant. We expect that both large and small viscosity ratio drops will be difficult to fragment. In the case of $\lambda < 0.01$, high capillary numbers are necessary to cause a transient elongation as very elongated steady shapes are possible (Figures 2 and 4). For $\lambda > O(10)$, highly stretched drops are capable of relaxing back to a spherical shape following cessation of the flow because of the significant internal flow resistance. Even for $\lambda = O(1)$, a deformation (L/a) approximately three times the maximum

steady deformation is necessary to ensure breakup; the fact that rather large deformations relative to the steady state shape are necessary to promote breakup was first indicated by Grace (1971).

One further observation that follows from the above experiments is that the initial fragmentation of the drop is controlled by global features of the shape, rather than being dependent on small scale, or local, features. However, local details of the shape, which vary with viscosity ratio, and the experimental details (e.g. asymmetries present in the initial configuration), affect the formation of satellite and subsatellite drops.

If the drop is stretched sufficiently, $L/a > O(20)$, then capillary waves, which grow to finite amplitude slowly owing to the small initial disturbances present in carefully controlled experiments, have time to evolve to a sufficiently large amplitude to affect the drop dynamics. In such circumstances, capillary waves play a significant, if not dominant, role in controlling the final drop size distribution (Tjahjadi & Ottino 1991); this behavior is commonly observed in polymer blending processes (e.g. Elemans 1989).

Finally, for step changes to subcritical conditions with $\mathbf{C} \neq 0$, it is possible to break drops without producing large-scale stretching of the drop. Such a model time-dependent flow is illustrated in the numerical simulations shown in Figure 7. The detailed velocity fields and transient drop shapes following a step change to 0.5 $\mathbf{C}_c$ are displayed in Figure 7*b*. Comparable experiments have also been performed (Stone & Leal 1989b). This manner of breakup adds just a few—though rather large and uniformly sized—drops to the drop size distribution. Also, it is possible to fragment very viscous drops in flows with significant vorticity (for example, a drop with $\lambda > 4$ in a simple shear flow), if the *initial deformation* is sufficiently large, as may be produced by first applying a low vorticity, high shear rate flow. An example is provided by Stone & Leal (1989b, Figure 13).

Complex Flows

It is worthwhile to consider more complicated flows, especially flows more representative of industrial applications. However, it is difficult to characterize three-dimensional flows in a manner that could be combined with fundamental studies of drop breakup to produce a useful picture of real mixing processes. Also, it remains a challenging numerical problem to describe even modest, low capillary number, three-dimensional distortions of drops in a simple shear flow. The reader interested in numerical investigations of three-dimensional drop deformation at low Reynolds numbers is referred to Rallison (1981), de Bruijn (1989), and Pozrikidis (1992). The calculation of the fragmentation of highly deformed drop shapes has not

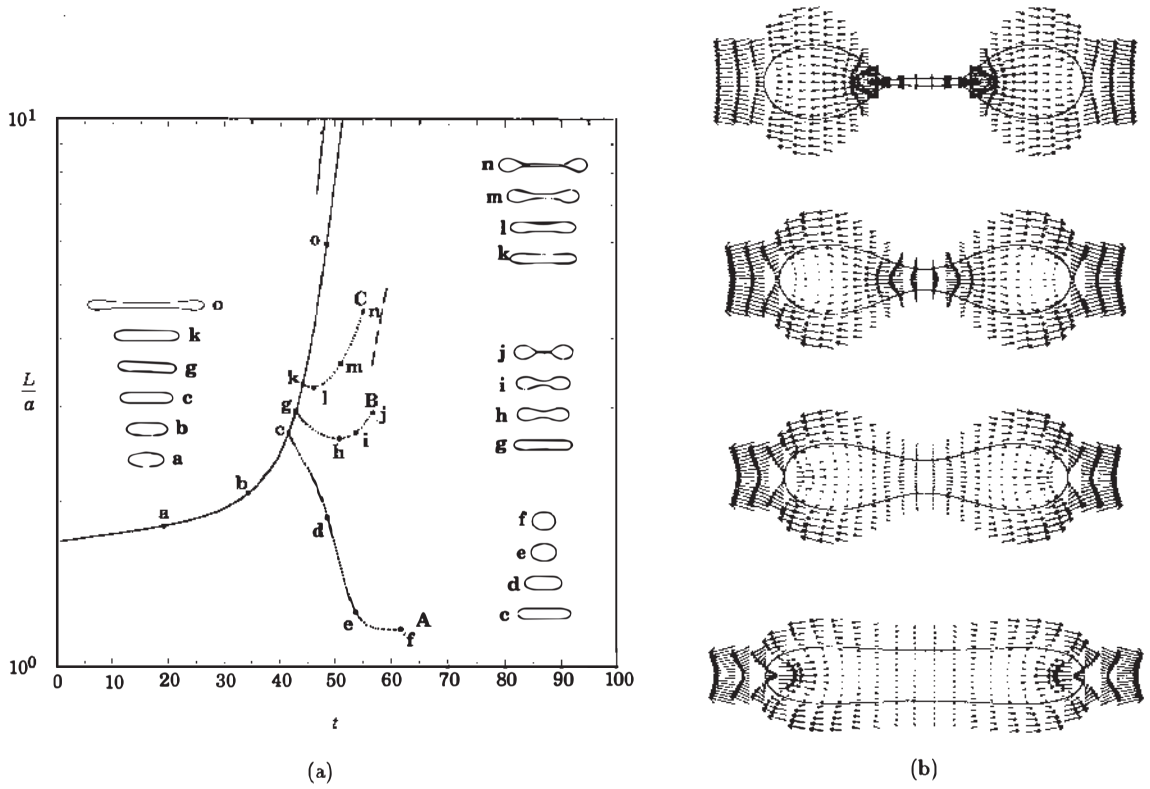

Figure 7 $\lambda = 1.0$; axisymmetric extensional flow. (*a*) Numerical simulations of step changes in capillary number from C_c to the subcritical value $0.5C_c$. The solid curve is the time-dependent stretching of the drop at the critical capillary number, while the three dashed curves illustrate the response to the step change. The solid (dashed) almost vertical line is the asymptotic limit of stretching like a fluid element in the original (subcritical) extensional flow. (*b*) The flow field and drop shape as a function of time following a step reduction in capillary number. The simulations correspond to the intermediate shapes shown along curve B in (*a*) (Stone & Leal 1989b).

yet been implemented satisfactorily. The two elements of (*a*) a complicated bulk flow and (*b*) dynamics of drop deformation, are in general coupled—the flow field from the Lagrangian view point of the drop will be time-dependent and perhaps changing on a time-scale comparable to the typical time for drop distortion, $a\mu(1+\lambda)/\gamma$.

Tjahjadi & Ottino (1991) present a first step towards bridging the gap between model studies of drop breakup and applications involving the mixing of immiscible viscous fluids. These authors describe an experimental investigation of the stretching and breakup of filaments in two-dimensional low Reynolds number chaotic flows generated via periodic modulation of the boundaries of an eccentric journal bearing apparatus. The time-dependent boundary motion is responsible for the appearance, in at least some part of the flow domain, of chaotic particle paths, which indicate that two nearby fluid particles separate exponentially in time for some (often large) range of initial conditions in the flow. In the experiments a fluid drop ($0.01 < \lambda < 2.8$) is placed in the chaotic region of the flow where the critical capillary number for breakup is exceeded. The drop is stretched rapidly into a slender filament, which then behaves as a passive tracer. The length of the thread-like shape generally increases exponentially with time, often reaching end-to-end stretches 10^3 times the initial drop radius. The final drop size distributions are also determined.

A typical example of the evolution of the drop, along with its subsequent fragmentation, is shown in Figure 8. Drop breakup primarily occurs as a result of capillary wave instabilities. Near the end of the filament and at intermediate locations where the filament is broken, end-pinching occurs producing rather large drops. The chaotic character of the flow produces *folds* in the filament, where at later times interfacial tension causes breakup again leading to large satellite drops.

A simplified model which assumes that the filament behaves passively in the flow accounts for the overall large-scale stretching. When combined with the linearized analysis for the growth of perturbations on cylindrical threads, the model can predict regions of potential breakup and approximate the size of the largest satellite drops. In the experiments, the lower viscosity ratio systems typically lead to more uniform drop size distributions since the breakup occurs rather quickly and the flow can generally break up the larger drops a second or third time (see also Figure 5*a*). For the higher viscosity ratio systems $\lambda > O(1)$, internal fluid motions required for breakup are damped, capillary instabilities thus occur less readily, and therefore the filament stretches and thins more prior to breakup. The small drops thus formed upon fragmentation of the thread are characterized by capillary numbers less than the critical value and hence do not typically break a second time. Breakup near folds and end-

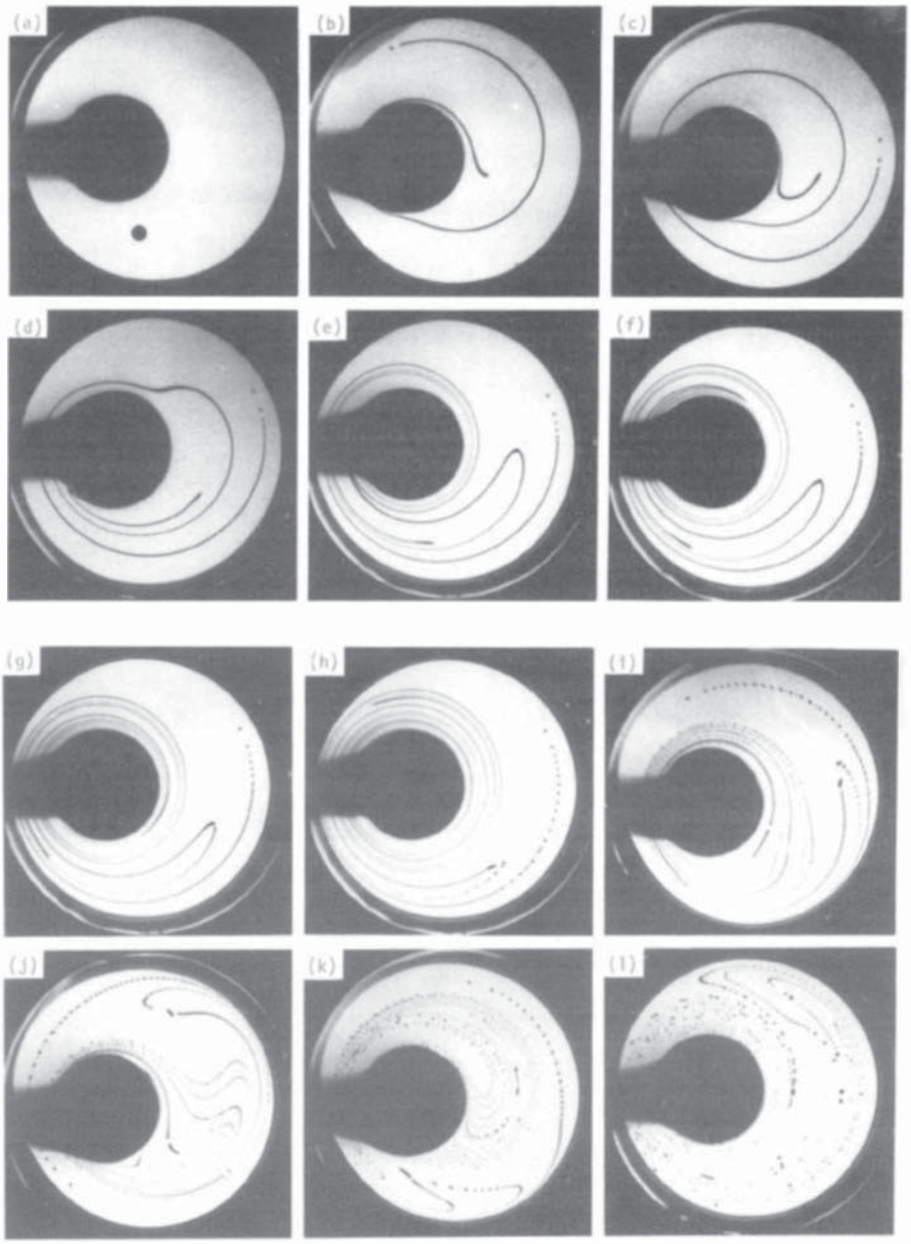

Figure 8 Dynamics of elongation, folding, and breakup of a drop placed in the globally chaotic flow produced in a time-periodically modulated eccentric journal bearing. The times corresponding to the different snapshots of the flow are given in the original publication. $\lambda = 0.067$ (Tjahjadi & Ottino 1991).

pinching lead to rather large drops that will likely fragment again. Overall, the experiments indicate that the drop size distribution in high viscosity ratio systems is more nonuniform, with a smaller mean drop size, than the lower viscosity ratio systems.

Satellite Drops

Drop or fluid filament fragmentation, whether by growth of capillary instabilities or via end-pinching because of the finite size of the drop, results in a distribution of drop sizes. In between the largest visible drops are smaller satellite drops and on still smaller scales there are subsatellite drops. There are, of course, similarities between the fragmentation of a viscous fluid filament and the breakup of weakly viscous fluid jets (Bogy 1979). Linear stability theory is unable to predict the existence of satellite drops and consequently, at least in its simplest form, provides no insight into the detailed evolution of the satellite drop size distribution.

Tjahjadi et al (1992) report a detailed study documenting satellite and subsatellite drop formation that result from the growth of capillary instabilities on the surface of a long, otherwise stationary, viscous fluid thread. In a set of experiments with viscosity ratios $0.01 < \lambda < 2.8$, fluid threads with radius 0.1 cm fragment; this leads to an array of smaller drops, where the smallest visible drops have radii of about 10 μm. The basic features of the breakup are illustrated in Figure 9. Complementary boundary integral calculations also shown in Figure 9 illustrate the small-scale flow and breakup processes (see Tjahjadi et al for a description of the numerical approximations introduced for treating the multiple breakup events). Linear stability theory for this viscous flow problem dates back to Tomotika (1935).

The viscosity ratio λ between the two fluids plays the most significant role in determining the eventual drop size distribution. For $\lambda > O(1)$, internal flow processes are damped leading to a smaller number of more uniformly sized drops, while for the smallest viscosity ratio studied, $\lambda = 10^{-2}$, many small satellites and subsatellites are formed between the largest mother drops. In general, the disturbance wavelength observed is within 20% of the optimum value predicted by linear stability theory on the basis of the largest disturbance growth rate.

For cases where drop breakup occurs in model chaotic flows, it appears that the drop size distribution generated at long times (i.e. after several splittings) can be described with a scaling analysis that yields the fraction of the population with a given radius (Muzzio et al 1991). The available experiments fall into two classes depending on whether $0.01 < \lambda < O(1)$ (experiments with smaller viscosity ratios were not performed) or whether $\lambda > O(1)$. The observation that the drop size distribution appears to be

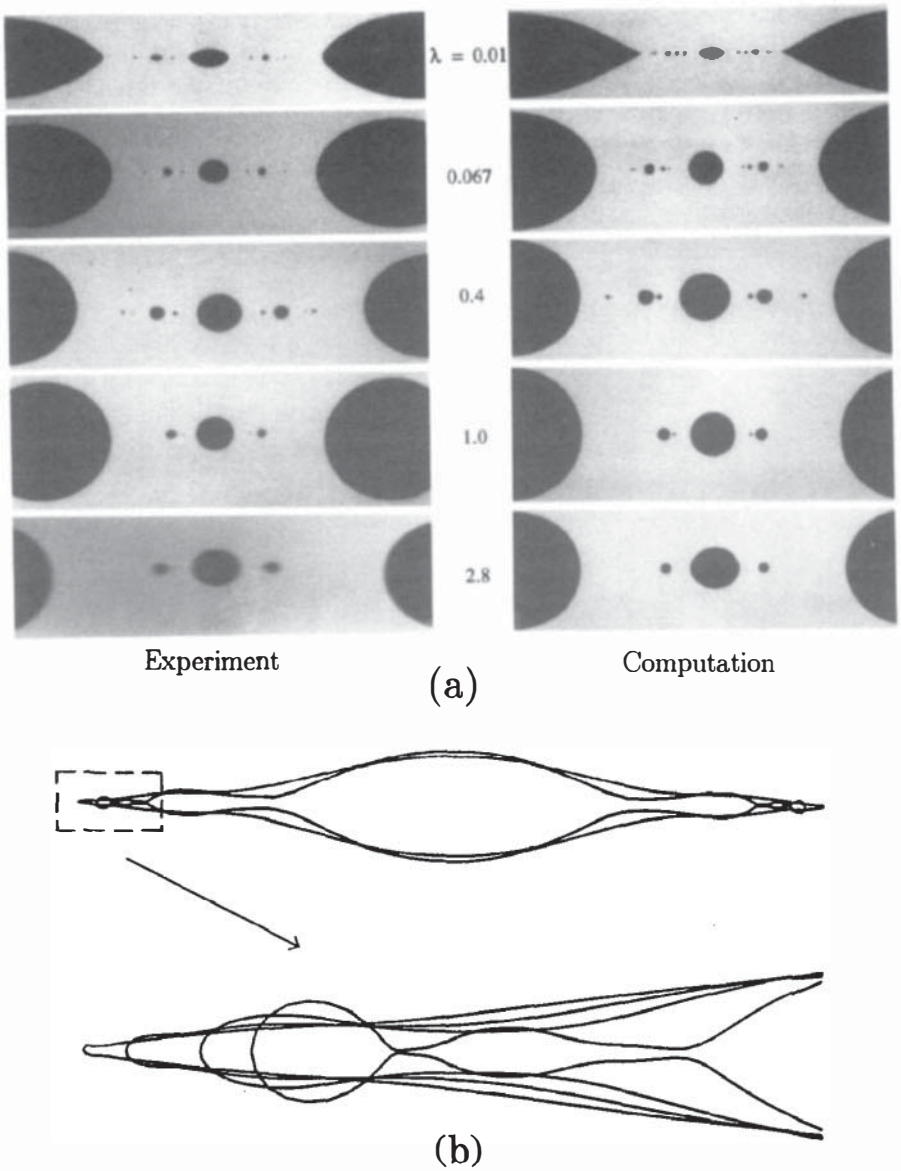

Figure 9 Breakup of a filament into satellite and subsatellite drops. (*a*) The effect of viscosity ratio. Shapes of the filament after the last fragmentation are shown. The dimensionless times at which the experiments and simulations are compared are within 4%. (*b*) Numerical simulation of the breakup of the narrow thread-like filament that appears between the large parent drops. An enlargement is shown illustrating the relaxation and breakup of the narrow end (Tjahjadi et al 1992).

controlled by the viscosity ratio has a relatively simple explanation. For the higher viscosity ratios, very large stretchings and thin threads are produced by the flow. Upon capillary fragmentation of the thread the small drops formed do not typically fragment a second time. On the other hand, the lower viscosity ratio systems fragment more quickly forming larger drops which thus undergo subsequent stretching and breakup.

Dynamical Analysis of Microstructured Fluids in Complex Flows

The detailed analysis of drop deformation and breakup in other complicated flows is formidable owing to the coupling of three-dimensional drop shapes with time-dependent velocity fields, as experienced by a drop as it traverses a given mixing device. Some progress is nevertheless possible if a model is introduced for the drop dynamics while maintaining complexity of the underlying flow field. A first step in this direction was made by Olbricht et al (1982) who introduced an evolution equation for a stretchable, orientable microstructure. In its simplest form the state of the microstructure is described by an axial vector which may be used for example to model the average length and orientation of a deforming droplet. This work establishes a strong flow criterion for steady flows which gives an estimate for the shear rate and flow conditions required to initiate stretching [see also Ottino (1990), Sections 9.3 and 9.4; and Khakhar & Ottino (1986), who discuss how the model vector equation may be interpreted to obtain the approximate dynamics of low viscosity ratio, highly stretched drops].

Szeri et al (1992) establish a strong flow criterion for the case of unsteady, spatially inhomogeneous flows which illustrates the effects of time dependence on the evolution of the microstructural element. Specifically, the vector model equation of Olbricht et al is used to describe the dynamics of a stretchable, orientable microstructure and is coupled to a time-dependent two-dimensional flow. The time evolution of the configuration of the microstructure is determined for time-periodic flows and the analysis takes advantage of several advances in understanding dynamical systems. A time-periodic flow history is experienced by a drop in a number of quite plausible circumstances, including recirculating particle paths in flows with closed streamlines, a steady flow in a spatially periodic domain, or a flow near a stagnation point that varies periodically in time.

Via several examples Szeri et al show that the neglect of time dependence may lead to incorrect characterization of the flow if instead the flow field is modeled by a sequence of steady states. An important assumption in the analysis is the neglect of any particle-particle interactions. Implications for stretched droplets are difficult to infer directly since at low capillary

numbers, interfacial tension plays an important role in the dynamics and introduces another time scale for the stretching dynamics.

Stretching of Thin Viscous Inclusions

The limit of zero interfacial tension is of practical significance to geophysical flow problems as well as to such industrial problems as glass manufacturing. The slender body analysis of the stretching of very viscous, neutrally buoyant inclusions has been presented by Spence et al (1988) and Wilmott (1989a,b). No steady drop shape is possible in these extensional fluid motions since there is nothing to resist the viscous stresses exerted on the inclusion by the external flow, and thus the inclusion stretches and thins on a time scale given approximately by the inverse shear rate G^{-1}. On this time scale the internal and external flows are coupled provided the slender inclusion, with slenderness ratio ε, is sufficiently viscous, i.e. $\lambda = O(\varepsilon^{-2})$ for axisymmetric inclusions and $\lambda = O(\varepsilon^{-1})$ for two-dimensional sheets. In general, the inclusion stretches exponentially, with small corrections from behavior identical to a fluid element owing to the viscosity contrast and finite inclusion length.

The analyses demonstrate analytically that an inclusion with smooth initial data cannot fragment in finite time, which is a result that might be expected owing to the absence of interfacial tension or any other destabilizing mechanism. For arbitrary initial shapes, it is shown how the slender inclusion will progressively thin; which may be useful for understanding the role of other effects, e.g. intermolecular forces that will become important at very short length scales (approximately 1000 Å).

5. EFFECTS OF SURFACTANTS

The presence of impurities has noticeable effects on the deformation of fluid-fluid interfaces simply because the impurities lower the interfacial tension. Also, surfactant gradients along the interface cause tangential stresses that produce fluid motions (Marangoni flows). Consequently, the presence of surfactants alters drop shapes and changes the critical capillary number for drop breakup. An experimental study by de Bruijn (1989, 1993) documents the importance of surfactants for explaining the phenomenon of tip streaming.

In this section, we summarize the effects of surfactants on the deformation and breakup of drops in externally imposed straining flows. It is assumed that the only effect of the surfactant is to modify the magnitude of the interfacial tension, which is quite reasonable provided the surfactant is present at low concentrations. Other interfacial rheological effects such as surface shear and dilatational viscosities are neglected (Edwards et al

1991). The surface rheology characteristic of thin elastic membranes is discussed, for example, by Li et al (1988).

The effects of surfactants on the motion of translating drops in unbounded fluids or in capillaries are well studied and will not be discussed here. A complete understanding of the influences of surfactants on the motion of fluid-fluid interfaces may require knowledge of interfacial transport processes since Stebe et al (1991) demonstrate the remobilization of a surfactant retarded interface in the limit where desorption kinetics and diffusion away from the interface are fast. Surfactants are also useful in the hydrodynamic modeling of cell cleavage (e.g. Greenspan 1978, Zinemanas & Nir 1988).

Deformation in Shear Flow

In order to quantify the effect of surfactants on free-boundary problems it is necessary to introduce a constitutive equation relating surfactant concentration Γ to the local value of interfacial tension γ. Typically, a linear equation of state is chosen with $\gamma(\Gamma)$ given by the two-dimensional gas law, $\gamma_s - \gamma = RT\Gamma$, where γ_s is the interfacial tension of a clean interface ($\Gamma = 0$), R is the gas constant, and T is the absolute temperature. Milliken et al (1993) have examined numerically some influences of a nonlinear equation of state on drop deformation and breakup. We let Γ_0 denote the (equilibrium) uniform surfactant concentration along the interface in the absence of flow; $\gamma_0 = \gamma_s - RT\Gamma_0$.

Surfactants have two independent effects on free-boundary motions. First, surfactants modify the mean interfacial tension, which alters the normal stress jump across the interface. A capillary number based upon a mean value of the interfacial tension $\mathsf{C}_0 = Ga\mu/\gamma_0$ is thus indicative of the degree of deformation caused by an external flow. Second, Marangoni stresses affect the fluid motion and produce a tangential stress jump. The dimensionless stress balance accounting for these two influences of surfactants is (we have chosen the characteristic velocity $u_c = Ga$)

$$\mathbf{n}\cdot\mathbf{T} - \lambda\mathbf{n}\cdot\hat{\mathbf{T}} = \frac{\gamma(\Gamma)/\gamma_0}{\mathsf{C}_0}(\nabla_s\cdot\mathbf{n})\mathbf{n} - \frac{\mathsf{B}_0}{\mathsf{C}_0}\hat{\mathbf{g}}\cdot\mathbf{x}\mathbf{n} + \frac{\beta}{\mathsf{C}_0\gamma_0/\gamma_s}\nabla_s(\Gamma/\Gamma_0) \quad \text{on } S, \tag{7}$$

where $\beta = -(d\gamma/d\Gamma)(\Gamma_0/\gamma_s)$ provides a dimensionless measure of interfacial tension variations produced by the surfactant. For the familiar two-dimensional gas law, $\beta = RT\Gamma_0/\gamma_s$. Here, B_0 is the Bond number based upon γ_0 (see Equation 2).

Predicting the degree of drop deformation in shear flows requires coupling the Stokes equations with equations describing surfactant transport

and the surface constitutive relation. Surfactant transport along the fluid-fluid interface is governed by a convective-diffusion equation (for a straightforward derivation see Stone 1990)

$$\frac{\partial(\Gamma/\Gamma_0)}{\partial t} + \nabla_s \cdot \left[\frac{\Gamma}{\Gamma_0} \mathbf{u}_s - \frac{1}{\mathbf{C}_0 \delta} \nabla_s \frac{\Gamma}{\Gamma_0} \right] + \frac{\Gamma}{\Gamma_0} (\nabla_s \cdot \mathbf{n})(\mathbf{u} \cdot \mathbf{n}) = j_n, \tag{8}$$

where $\mathbf{u}_s$ is the velocity vector directed tangent to the surface, j_n is the dimensionless net flux of surface-active material to and from the surface, $\delta = \gamma_0 a/(\mu D_s)$, and D_s is the surface diffusivity. The surface Péclet number is $\mathbf{C}_0\delta$.

Drop deformation now depends on $\mathbf{C}_0$, λ, β (i.e. the constitutive equation), and δ. From a theoretical viewpoint, not only must a free-boundary problem be considered, but the presence of surfactants complicates the calculation further, since their distribution is coupled to the drop shape, which, of course, depends upon the detailed surfactant distribution. In the simplest case the surfactant is treated as insoluble ($j_n = 0$), which is a useful approximation when most of the surfactant resides along the interface (as expected at low concentrations for cases such that the partition coefficient favors surface adsorption). The study of insoluble surfactant and the analogous clean interface problem thus provide bounds for the possible interface distortions. If surfactant resides in the bulk fluids, then additional transport equations are required and boundary conditions are needed relating the surface and bulk concentrations (e.g. Stebe et al 1991).

The qualitative deformation behavior of drops in extensional flows can be understood by accounting for (*a*) ***convection*** of surfactant toward stagnation points at the end of the drop—this tends to lower interfacial tension, hence tends to increase the observed deformation; (*b*) ***dilution*** of surfactant owing to increased interfacial area which accompanies drop deformation—this tends to increase the interfacial tension, hence acts to decrease the observed deformation; and (*c*) additional ***adsorption*** and ***desorption*** of surfactant to and from the surface owing to fluxes from the bulk phases as deformation increases interfacial area.

Items (*a*) and (*b*) are discussed by Stone & Leal (1990). Because surface Péclet numbers are typically large (small surface diffusivities), convective transport effects dominate the surfactant distribution so deformation is enhanced over the uniform surfactant, or clean interface, case. Also, items (*b*) and (*c*) tend to offset one another. Nevertheless, if the time-scale characteristic of adsorption k_a is long compared with both G^{-1} and $(1+\lambda)\mu a/\gamma_0$, it may be expected that dilution effects play a more prominent role, tending to inhibit drop deformation.

SMALL DEFORMATION ANALYSIS An analysis of nearly spherical drop shapes ($\mathsf{C}_0 \ll 1$) was performed by Flumerfelt (1980), who incorporated interfacial shear and dilatational viscosities, and an accompanying experimental study was presented by Phillips et al (1980). Stone & Leal (1990) also considered the near-sphere limit analytically as part of a numerical investigation of finite drop deformation. Assuming that the deformation is small and the concentration of surfactant is nearly uniform (low surface Péclet numbers), the leading order deformation of the drop D may be calculated as (Stone & Leal 1990)

$$D \approx \frac{3\mathsf{C}_0 b_r}{4 + \mathsf{C}_0 b_r} \quad \text{where} \quad b_r = \frac{5}{4}\frac{(16+19\lambda)+4\beta\delta/(1-\beta)}{10(1+\lambda)+2\beta\delta/(1-\beta)}. \tag{9}$$

This equation reduces to Taylor's (1932) well-known result in the limits $\beta \to 0$ or $\delta \to 0$, which correspond, respectively, to no effect of surfactant on the interfacial tension or a uniform distribution of surfactant as convective effects are weak.

Drop deformation increases as the magnitude of b_r increases, which occurs at a fixed dimensionless shear rate C_0 if δ increases or β increases. In the small deformation analysis, the effect of surfactant convection appears via the combined parameter $\beta\delta/(1-\beta)$, which is proportional to the magnitude of the interfacial tension variations. The flow convects surfactant toward the end of the drop, resulting in a higher surfactant concentration and lower interfacial tension, thus requiring larger deformations to balance viscous forces.

NUMERICAL STUDIES Stone & Leal (1990) present a numerical study of surfactant effects on finite drop deformation in extensional flows. In particular, for the case of the insoluble surfactant it is demonstrated that dilution of the local surface concentration, owing to increases in interfacial area, may produce situations where the interfacial tension is actually higher than its original value and consequently further deformation, leading to breakup, tends to be inhibited. Also, the critical capillary number for breakup $(\mathsf{C}_0)_c$ is calculated as a function of the two dimensionless parameters, β and δ. Milliken et al (1993) have extended this study to examine the manner in which surfactants alter the transient motion of elongating drops and the relaxation of initially stretched drops. Generally, Marangoni stresses reduce the interfacial velocity and cause the drop to behave as if it has a higher viscosity. Surfactant effects are more pronounced at smaller viscosity ratios, $\lambda < 1$, generally producing drop shapes that have higher curvatures than in the absence of surfactants. This behavior is suggestive of the tip streaming phenomenon (tip streaming, however, was not observed in the numerical simulations), which is now discussed in detail.

Tip Streaming

Several experiments (Taylor 1934, Grace 1971) show that a low viscosity ratio drop, typically $\lambda < O(0.1)$, may establish a steady deformation with a shape that has nearly pointed ends, yet very small drops are ejected from the ends. The ejected drops typically have radii less than 50 μm. This behavior is called "tip streaming." Because of the generation of large numbers of very small droplets, it is of interest to understand what factors control this phenomenon. The tip streaming phenomenon was unresolved at the time of the earlier reviews of Acrivos (1983) and Rallison (1984).

Recently, de Bruijn (1989, 1993), via a comprehensive and careful set of experiments, has shed light on this subject. A convincing qualitative explanation is presented describing tip streaming as the result of surfactants being swept toward the narrow ends of the drop, so that at high enough surface concentrations the ends become rigid and viscous stresses tear the narrow end regions away. A corresponding theoretical description or numerical simulation is still lacking however.

De Bruijn (1989) documents most of the experimental references to tip streaming. An important observation is that this behavior only occurs for $\lambda < 0.1$. Also, tip streaming occurs for capillary numbers lower than $\mathbf{C}_c$ and when surfactant is purposefully added to the system, tip streaming is generally (though not always) observed.

The main conclusions to be drawn from de Bruijn's experimental study are:

1. Contrary to studies reporting that tip streaming stops due to a decrease in drop volume, the actual volume changes are too small for this to be true. It appears that tip streaming stops when most of the surfactant on the interface is swept away.
2. Controlled addition of surfactant leads to tip streaming for $\lambda < O(0.1)$ provided the surfactant concentration is large enough. However, surface impurity concentrations that are too high also inhibit tip streaming and the drop breaks by the usual mode, presumably because the interface is uniformly covered.
3. Inferred interfacial tensions of the small tip droplets (determined using a small deformation experiment) are lower, often much lower, than the interfacial tension of the original mother drop. The corresponding surfactant concentrations are close to the saturation value.

As a final note, Milliken & Leal (1991) observed tip streaming in an experimental study of the deformation of viscoelastic drops in extensional flows. Viscoelastic materials are often made by dissolving a small amount of a polymer in water or some other solvent. The polymers modify the

bulk rheology, but may also exhibit a tendency to accumulate along the interface due to the different chemical interactions of the polymer with the two bulk fluids. In Milliken & Leal's experiments with viscoelastic drops, tip streaming was observed when the Deborah number was larger than one and the viscosity ratio was small (the Deborah number is the ratio of the fluid relaxation time to the flow time scale). Hence, it appears likely that the tip streaming may be a consequence of the polymer acting as a surfactant rather than being caused by some modification of the bulk rheology (Milliken et al 1993).

6. INSTABILITY OF TRANSLATING DROPS

We have discussed in detail deformation in flows where the drops have been assumed to be neutrally buoyant ($B = 0$). Buoyancy-driven translation of spherical drops at low Reynolds numbers has been studied extensively. In this section we summarize studies, which have been reported only recently, of the stability and flow-induced deformation of nonspherical drop shapes.

When a spherical drop of one fluid undergoes low Reynolds number buoyancy-driven translation through a second fluid, the translational velocity is higher than that of the equivalent rigid sphere by the factor $3(1+\lambda)/(2+3\lambda)$. The Hadamard-Rybczyński flow field is derived using the Stokes equations to describe the velocity field in both fluid phases, along with the boundary conditions of continuity of velocity and tangential stress. The solution is remarkable in that the normal stress boundary condition is satisfied identically, as the pressure and viscous forces are in exact balance everywhere along the interface, and this result is independent of the magnitude of the interfacial tension (including zero interfacial tension). Hence, a spherical shape is an exact steady solution to the low Reynolds number drop translation problem (Batchelor 1967).

Translation in Unbounded Fluids

The shape evolution of nonspherical drops in simple translation was first examined by Kojima et al (1984). Using a linear stability analysis, these authors show that (*a*) in the absence of interfacial tension the spherical shape is ***unstable*** to infinitesimal disturbances and (*b*) at finite Bond numbers the drop will recover a steady spherical shape provided that the initial nonspherical distortion is not too large (the Bond number and capillary number are equivalent for buoyancy-driven flows). When an instability is predicted to occur, the analysis demonstrates that perturbations near the front stagnation point are diminished in amplitude due to the local elongational flow, thus returning the front of the drop to a spherical shape. Perturbations near the rear stagnation point are amplified

in a manner which suggests (*i*) the formation of a tail for initially prolate distortions and (*ii*) the formation of a dimple, or cavity, for initially oblate distortions. The question of whether these conclusions carry over to the case of finite initial deformation has been examined in detail via numerical boundary integral calculations by Koh & Leal (1989) and Pozrikidis (1990).

Koh & Leal (1989) present an investigation of the critical initial deformation beyond which no steady spherical shape is possible and thus the drop undergoes continuous distortion. The axisymmetric initial shapes are chosen to be either oblate or prolate ellipsoids of revolution. A companion experimental study (Koh & Leal 1990) shows that the numerical results are in excellent agreement with laboratory observations which allows the further conclusion that provided global shape information is given, then the evolution of the interface shape can be predicted. Pozrikidis (1990) presents a careful study of the limit of vanishing interfacial tension; very large distortions typified by either long tails or large cavities are common in this limit. Numerical simulations showing typical shape evolutions characteristic of different Bond numbers and viscosity ratios are shown in Figure 10 for sedimenting drops.

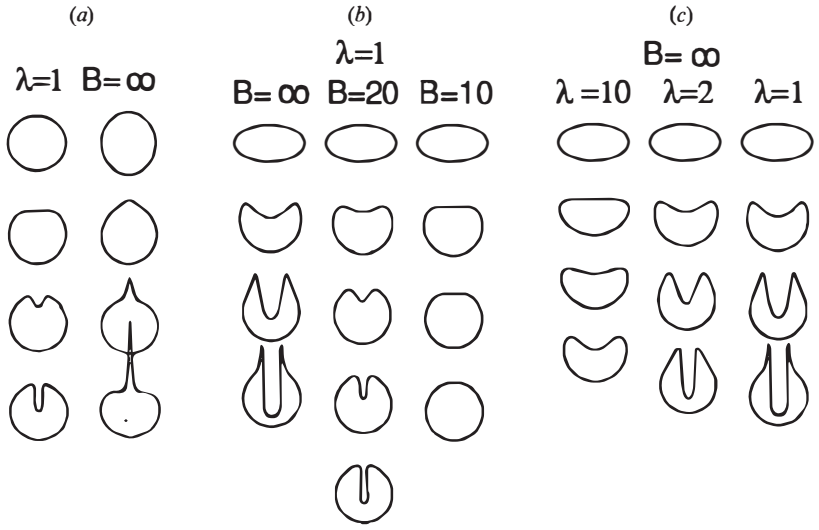

Figure 10 Buoyancy-driven motion and instability of sedimenting drops. (*a*) A slightly nonspherical oblate (prolate) initial shape translates and evolves a cavity (tail). The interfacial tension is zero. (*b*) The effect of interfacial tension on the stability of an initially oblate drop shape. For sufficiently strong interfacial tension ($B \lesssim 10$) the drop recovers a spherical shape, while drops with lower interfacial tensions develop cavities. (*c*) The effect of viscosity ratio on the evolution of oblate initial shapes. (Numerical computations performed by M. Manga.)

Overall, we see a connection with drop deformation in extensional flows: For each nonzero Bond number, there is a critical initial distortion such that the drop is unable to recover the spherical shape, and so deforms continuously (this defines a critical Bond number). In particular, sufficiently distorted prolate shapes evolve into drops with nearly spherical fronts and long narrow tails. Initially oblate shapes develop large cavities at the back with the internal circulatory flow causing the cavity to continually increase in depth until it approaches the front interface; a nearly steady ring shape, or torus, is thus formed. In the experiments of Koh & Leal (1990), oblate drops that evolve cavities eventually close upon themselves, encapsulating the continuous phase fluid, and form double emulsion drop. Qualitatively the viscosity ratio has only a small influence on the evolution (and stability) of prolate shapes. However, for oblate shapes that evolve cavities, the higher the viscosity ratio (thus higher internal viscous stresses), the lower the critical Bond number for instability.

In the original experiments of Kojima et al (1984) the drops develop cavities and rapidly evolve into a toroidal shape with the radius of the torus increasing with time. An analysis incorporating inertial effects was proposed to explain this observation.

Other Driving Forces

Thermocapillary migration of drops in a temperature gradient occurs owing to the temperature dependence of the interfacial tension. For this flow situation, Ascoli & Lagnado (1992) use a linear stability analysis to show that a spherical drop shape may also be unstable to infinitesimal perturbations even if the interfacial tension is finite. The instability is a consequence of the interfacial tension gradient that accompanies the nonuniform temperature field. For properties characteristic of air bubbles in silicon fluids, the temperature gradients required to produce instability of centimeter-sized bubbles is estimated to be 200°C cm^{-1}, a rather unrealistic value. The effect of finite distortions, which requires a numerical solution, has not been examined, so may yet show that moderate temperature gradients can produce instability of finitely distorted drops. The corresponding problem of translation of dielectric fluid drops in nonuniform electric fields has not been examined.

7. CONCLUSIONS

The subject of drop deformation in viscous flows has found recent application in a large number of diverse disciplines (Table 1) spanning a wide range of length scales. A common theme of research during the past ten years has been the understanding of (*a*) transients leading to drop

fragmentation and (*b*) drop deformation for systems containing surfactants or characterized by more complex surface rheologies.

Future research directions are difficult to anticipate. One important and challenging problem which awaits an adequate solution is to incorporate the basic elements of the research described here into a model of a viscous multiphase flow containing a large number of dispersed droplets, with the goal to predict accurately the drop size distribution. A first step in this direction was taken by Tjahjadi & Ottino (1991)—see Section 4. The incorporation of microscale dynamics into a global, or large scale, model of a dispersed multiphase flow is now appropriate, not the least because many of the research problems described in the drop breakup literature are motivated at least in part by industrial processes. A useful model should include the possibility of coalescence of two drops in the presence of shear, a problem which is not well understood at this time. A second area where drop deformation and breakup studies may prove useful is the quantitative analysis of the motion and deformation of drops in complex media, such as fibrous beds or other porous materials. In this case the drop experiences a time-dependent shear and extensional motion as it passes through the pore space (this problem area was described to the author by E. S. G. Shaqfeh). A third area that deserves more attention, notably because many practical problems involve polymeric dispersed materials, includes both the response of viscoelastic drops to shear and an improved understanding of how the dynamics of breakup are affected by a viscoelastic continuous phase.

ACKNOWLEDGMENTS

I would like to thank E. J. Hinch, L. G. Leal, M. Manga, J. M. Ottino, J. M. Rallison, J. D. Sherwood, and M. Tjahjadi for providing a critical reading of the original version of this paper. Their penetrating remarks and suggestions led to a large number of improvements in the final version of the manuscript. Also, I am thankful to B. J. Bentley and W. J. Milliken for their collaborations on some of the work reported here. E. J. Hinch is thanked for initially describing de Bruijn's research to me and M. Manga is thanked for performing the numerical simulations shown in Figure 10. Finally, I would like to thank the National Science Foundation for their support of this project and the editors of Annual Reviews for their patience.

Literature Cited

Acrivos, A. 1983. The breakup of small drops and bubbles in shear flows. *4th Int Conf. on Physicochemical Hydrodynamics, Ann. N. Y. Acad. Sci.* 404: 1–11

Acrivos, A., Lo, T. S. 1978. Deformation and breakup of a single slender drop in an extensional flow. *J. Fluid Mech.* 86: 641–72

Ascoli, E. P., Lagnado, R. R. 1992. The linear stability of a spherical drop migrating in a vertical temperature gradient. *Phys. Fluids A* 4: 225–33

Barthès-Biesel, D., Acrivos, A. 1973. Deformation and burst of a liquid droplet freely suspended in a linear shear field. *J. Fluid Mech.* 61: 1–21

Batchelor, G. K. 1967. *An Introduction to Fluid Dynamics.* Cambridge: Cambridge Univ. Press. 615 pp.

Bentley, B. J., Leal, L. G. 1986a. A computer-controlled four-roll mill for investigations of particle and drop dynamics in two-dimensional linear shear flows. *J. Fluid Mech.* 167: 219–40

Bentley, B. J., Leal, L. G. 1986b. An experimental investigation of drop deformation and breakup in steady two-dimensional linear flows. *J. Fluid Mech.* 167: 241–83

Bogy, D. B. 1979. Drop formation in a circular liquid jet. *Annu. Rev. Fluid Mech.* 11: 207–28

Buckmaster, J. D. 1972. Pointed bubbles in slow viscous flow. *J. Fluid Mech.* 55: 385–400

Carriere, C. J., Cohen, A., Arends, C. B. 1989. Estimation of interfacial tension using shape evolution of short fibers. *J. Rheol.* 33: 681–89

de Bruijn, R. A. 1989. *Deformation and breakup of drops in simple shear flows.* PhD thesis. Tech. Univ. Eindhoven. 274 pp.

de Bruijn, R. A. 1993. Tipstreaming of drops in simple shear flows. *Chem. Eng. Sci.* 48: 277–84

Döring, M. 1982. Ink-jet printing. *Philips Tech. Rev.* 40: 192–98

Edwards, D. A., Brenner, H., Wasan, D. T. 1991. *Interfacial Transport Processes and Rheology.* Boston: Butterworth-Heinemann. 558 pp.

Elemans, P. H. M. 1989. *Modelling of the processing of incompatible polymer blends.* PhD thesis. Tech. Univ. Eindhoven. 207 pp.

Elemans, P. H. M., Janssen, J. M. H., Meijer, H. E. H. 1990. The measurement of interfacial tension in polymer/polymer systems: the breaking thread method. *J. Rheol.* 34: 1311–25

Flumerfelt, R. W. 1980. Effects of dynamic interfacial properties on drop deformation and orientation in shear and extensional flow fields. *J. Colloid Interface Sci.* 76: 330–49

Giesekus, H. 1962. Strömungen mit konstantem Geschwindigkeitsgradienten und die Bewegung von darin suspendierten Teilchen. Teil II: Ebene Strömungen und eine experiementelle Anordnung zu ihrer Realisierung. *Rheol. Acta* 2: 113–21

Grace, H. P. 1971. Dispersion phenomena in high viscosity immiscible fluid systems and application of static mixers as dispersion devices in such systems. *Eng. Found., Res. Conf. Mixing, 3rd, Andover, N. H.* Republished in 1982 in *Chem. Eng. Commun.* 14: 225–77

Greenspan, H. P. 1978. On fluid-mechanical simulations of cell division and movement. *J. Theoret. Biol.* 70: 125–34

Hakimi, F. S., Schowalter, W. R. 1980. The effects of shear and vorticity on deformation of a drop. *J. Fluid Mech.* 98: 635–45

Han, C. D. 1981. *Multiphase Flow in Polymer Processing.* New York: Academic

Hinch, E. J., Acrivos, A. 1979. Steady long slender droplets in two-dimensional straining motion. *J. Fluid Mech.* 91: 401–14

Jeong, J.-T., Moffatt, H. K. 1992. Free-surface cusps associated with flow at low Reynolds number. *J. Fluid Mech.* 241: 1–22

Joseph, D. D., Nelson, J., Renardy, M., Renardy, Y. 1991. Two-dimensional cusped interfaces. *J. Fluid Mech.* 223: 383–409

Khakhar, D. V., Ottino, J. M. 1986. A note on the linear vector model of Olbricht, Rallison, and Leal as applied to the breakup of slender axisymmetric drops. *J. Non-Newtonian Fluid Mech.* 21: 121–27

Koh, C. J., Leal, L. G. 1989. The stability of drop shapes for translation at zero Reynolds number through a quiescent fluid. *Phys. Fluids A* 1: 1309–13

Koh, C. J., Leal, L. G. 1990. An experimental investigation on the stability of viscous drops translating through a quiescent fluid. *Phys. Fluids A* 2: 2103–9

Kojima, M., Hinch, E. J., Acrivos, A. 1984. The formation and expansion of a toroidal drop moving in a viscous fluid. *Phys. Fluids* 27: 19–32

Kuiken, H. K. 1990. Viscous sintering: the surface-tension-driven flow of a liquid form under the influence of curvature gradients at its surface. *J. Fluid Mech.* 214: 503–15

Levich, V. G., Krylov, V. S. 1969. Surface-tension-driven phenomena. *Annu. Rev. Fluid Mech.* 1: 293–316

Li, X. Z., Barthès-Biesel, D., Helmy, A. 1988. Large deformations and burst of a capsule freely suspended in an elongational flow. *J. Fluid Mech.* 187: 179–96

Meijer, H. E. H., Janssen, J. M. H. 1993. Mixing of immiscible liquids. In *Mixing and Compounding—Theory and Practice*, ed. I. Mana-Zloczower, Z. Tadmor, Pro-

gress in Polymer Processing Ser. Munich: Carl Hanser

Mikami, T., Cox, R. G., Mason, S. G. 1975. Breakup of extending liquid threads. *Int. J. Multiphase Flow* 2: 113–38

Milliken, W. J., Leal, L. G. 1991. Deformation and breakup of viscoelastic drops in planar extensional flows. *J. Non-Newtonian Fluid Mech.* 40: 355–79

Milliken, W. J., Stone, H. A., Leal, L. G. 1993. The effect of surfactant on the transient motion of Newtonian drops. *Phys. Fluids* 5: 69–79

Muzzio, F. J., Tjahjadi, M., Ottino, J. M. 1991. Self-similar drop-size distributions produced by breakup in chaotic flows. *Phys. Rev. Lett.* 67: 54–7

Olbricht, W. L., Rallison, J. M., Leal, L. G. 1982. Strong flow criteria based on microstructure deformation. *J. Non-Newtonian Fluid Mech.* 10: 291–318

Ottino, J. M. 1990. *The Kinematics of Mixing: Stretching, Chaos and Transport.* Cambridge: Cambridge Univ. Press. 364 pp.

Phillips, W. J., Graves, R. W., Flumerfelt, R. W. 1980. Experimental studies of drop dynamics in shear fields: role of dynamic interfacial effects. *J. Colloid Interface Sci.* 76: 350–70

Pozrikidis, C. 1990. The instability of a moving viscous drop. *J. Fluid Mech.* 210: 1–21

Pozrikidis, C. 1992. *Boundary Integral and Singularity Methods for Linearized Viscous Flow.* Cambridge: Cambridge Univ. Press. 259 pp.

Rallison, J. M. 1980. Note on the time-dependent deformation of a viscous drop which is almost spherical. *J. Fluid Mech.* 98: 625–33

Rallison, J. M. 1981. A numerical study of the deformation and burst of a viscous drop in general shear flows. *J. Fluid Mech.* 109: 465–82

Rallison, J. M. 1984. The deformation of small viscous drops and bubbles in shear flows. *Annu. Rev. Fluid Mech.* 16: 45–66

Rumscheidt, F. D., Mason, S. G. 1961. Particle motions in sheared suspensions. XII. Deformation and burst of fluid drops in shear and hyperbolic flow. *J. Colloid Sci.* 16: 238–61

Seward III, T. P. 1974. Elongation and spheroidization of phase-separated particles in glass. *J. Non-Crystalline Solids* 15: 487–504

Sherwood, J. D. 1981. Spindle-shaped drops in a viscous extensional flow. *Math. Proc. Cambridge Philos. Soc.* 90: 529–36

Sherwood, J. D. 1984. Tip streaming from slender drops in a nonlinear extensional flow. *J. Fluid Mech.* 144: 281–95

Skalak, R., Özkaya, N., Skalak, T. C. 1989. Biofluid mechanics. *Annu. Rev. Fluid Mech.* 21: 167–204

Spence, D. A., Ockenden, J. R., Wilmott, P., Turcotte, D. L., Kellogg, L. H., 1988. Convective mixing in the mantle: the role of viscosity differences. *Geophys. J.* 95: 79–86

Stebe, K. J., Lin, S.-Y., Maldarelli, C. 1991. Remobilizing surfactant retarded fluid particle interfaces. I. Stress-free conditions at the interfaces of micellar solutions of surfactants with fast sorption kinetics. *Phys. Fluids* 3: 3–20

Stone, H. A. 1990. A simple derivation of the time-dependent convective-diffusion equation for surfactant transport along a deforming interface. *Phys. Fluids A* 2: 111–12

Stone, H. A., Bentley, B. J., Leal, L. G. 1986. An experimental study of transient effects in the breakup of viscous drops. *J. Fluid Mech.* 173: 131–58

Stone, H. A., Leal, L. G. 1989a. Relaxation and breakup of an initially extended drop in an otherwise quiescent fluid. *J. Fluid Mech.* 198: 399–427

Stone, H. A., Leal, L. G. 1989b. The influence of initial deformation on drop breakup in subcritical time-dependent flows at low Reynolds numbers. *J. Fluid Mech.* 206: 223–63

Stone, H. A., Leal, L. G. 1990. The effects of surfactants on drop deformation and breakup. *J. Fluid Mech.* 220: 161–86

Szeri, A. J., Wiggins, S., Leal, L. G. 1991. On the dynamics of suspended microstructure in unsteady, spatially inhomogeneous, two-dimensional fluid flows. *J. Fluid Mech.* 228: 207–41

Taylor, G. I. 1932. The viscosity of a fluid containing small drops of another fluid. *Proc. R. Soc. London Ser. A* 138: 41–48

Taylor, G. I. 1934. The formation of emulsions in definable fields of flow. *Proc. R. Soc. London Ser. A* 146: 501–23

Taylor, G. I. 1964. Conical free surfaces and fluid interfaces. *Proc. Int. Congr. Appl. Mech., 11th, Munich,* pp. 790–96

Tjahjadi, M., Ottino, J. M. 1991. Stretching and breakup of droplets in chaotic flows. *J. Fluid Mech.* 232: 191–219

Tjahjadi, M., Stone, H. A., Ottino, J. M. 1992. Satellite and subsatellite formation in capillary breakup. *J. Fluid Mech.* 243: 297–317

Tjahjadi, M., Stone, H. A., Ottino, J. M. 1993. Estimating interfacial tension via relaxation of moderately extended droplets and breakup of highly extended fluid filaments. *AIChE J.* In press

Tomotika, S. 1935. On the stability of a cylindrical thread of a viscous liquid surrounded by another viscous fluid. *Proc. R. Soc. London Ser. A* 150: 322–37

Wilmott, P. 1989a. The stretching of a thin viscous inclusion and the drawing of glass sheets. *Phys. Fluids A* 1: 1098–103

Wilmott, P. 1989b. The stretching of a slender, axisymmetric, viscous inclusion—Part I: Asymptotic analysis. *SIAM J. Appl. Math.* 49: 1608–16

Zinemanas, D., Nir, A. 1988. On the viscous deformation of biological cells under anisotropic surface tension. *J. Fluid Mech.* 193: 217–41